DOI: 10.1002/ejoc.201101392

Photolytic Release of Butyric Acid from Oxygen- and Nitrogen-Based Heteroaromatic Cages

Ana M. S. Soares,[a] Ana M. Piloto,[a] Graham Hungerford,[b] Susana P. G. Costa,[a] and M. Sameiro T. Gonçalves*[a]

Keywords: Prodrugs / Butyric acid / Oxazoles / Oxobenzopyran / Coumarin / Photolysis / Fluorescence spectroscopy

In order to develop butyric acid photoactive prodrugs, new heteroaromatic conjugates based on oxygen and nitrogen were synthesised and evaluated under irradiation at 254, 300, 350 and 419 nm. Light-triggered uncaging of butyric acid from the corresponding heterocyclic cages was achieved with complete release of the drug in short times. Naphtho[2,3-*d*]oxazole, naphtho[1,2-*d*]oxazole, 3-oxo-3*H*-benzo[*f*]benzopyran, 2-oxo-2*H*-benzo[*h*]benzopyran and 6-oxo-6*H*-benzopyrano[6,7-*d*]oxazole conjugates were readily photolysed, and the best results were obtained for naphthooxazoles at 254 and 300 nm and for 3-oxo-3*H*-benzo[*f*]benzopyran, 2-oxo-2*H*-benzo[*h*]benzopyran and 2-methyl-6-oxo-6*H*-benzopyrano[6,7-*d*]oxazole at 350 nm. 3-Oxo-3*H*-benzo[*f*]benzopyran also afforded good results at 419 nm. The photophysical processes involved were further elucidated by the use of time-resolved fluorescence techniques.

Introduction

Several strategies for the development of pharmacologically inert chemical derivatives, prodrugs, which can be converted into active drug molecules, have been explored to overcome common drawbacks such as low oral drug absorption, lack of site specificity, chemical instability, toxicity and poor patient acceptance.[1–3] Photoactive prodrugs with a suitable photolabile group, whose reactivity can be controlled by selecting the wavelength of the excitation light, could be an alternative to the molecular design of prodrugs. The timed and accurate delivery of a drug at a specific location in vivo or in vitro presents a challenging goal that can be achieved by using photoactive prodrugs that are able to decompose rapidly upon photoirradiation. In recent reports in the field of prodrugs, there have been some examples of light as the triggering agent for the optimisation of drug delivery.[4–6] Given the promising results obtained, this strategy could allow for a more patient-friendly drug delivery and availability scheme, which involves less complex dosing schedules and a lower potential for side effects.

Drugs that contain ionisable polar groups such as carboxylic acids are poorly absorbed from the gastrointestinal tract due to lipophilicity/solubility issues. The absorption can be improved by masking the carboxyl group by forming derivatives through different covalent linkages.[1] Butyric acid is a naturally occurring short-chain fatty acid involved in the regulatory mechanisms for gene expression known to promote markers of cell differentiation, apoptosis and cell-growth control.[7,8] Prodrugs based on butyric acid, upon intracellular hydrolytic degradation, release acids and aldehydes, modulate gene expression, and induce histone hyperacetylation, differentiation and apoptosis of cancer cells. Prodrugs that release formaldehyde increase apoptosis of cancer cells, at concentrations about 10-fold lower than butyric acid and 100 times faster. The formaldehyde released from these prodrugs has been shown to be a critical antiproliferative factor that induces differentiation and cell death.[8–11]

Our recent research has focussed on the synthesis and application of new oxygen and nitrogen heterocycles as photosensitive groups for the protection of carboxylic acid and amino groups.[12–18] In order to extend the scope of applications of such groups to drug-delivery research in the form of photoactive prodrugs, this work evaluates the use of naphtho[2,3-*d*]oxazole, naphtho[1,2-*d*]oxazole, 3-oxo-3*H*-benzo[*f*]benzopyran, 2-oxo-2*H*-benzo[*h*]benzopyran and 6-oxo-6*H*-benzopyrano[6,7-*d*]oxazoles in the light-triggered release of butyric acid from the corresponding heterocyclic cages. The stability to irradiation of the ester bond between butyric acid and the caging group has been evaluated in a photochemical reactor at 254, 300, 350 and 419 nm, and uncaging data have been acquired. The photophysical processes involved have been further elucidated by the use of time-resolved fluorescence techniques.

Results and Discussion

The synthesis of bromomethylated naphtho[1,2-*d*]oxazole (**2**) was achieved by a condensation reaction between

[a] Centre of Chemistry, University of Minho, Campus of Gualtar, 4710-057 Braga, Portugal
Fax: +351-253604382
E-mail: msameiro@quimica.uminho.pt
[b] HORIBA Jobin Yvon IBH Ltd, 45 Finnieston Street, Glasgow G3 8JU, UK

Supporting information for this article is available on the WWW under http://dx.doi.org/10.1002/ejoc.201101392.

1-aminonaphthalen-2-ol and bromoethanoic acid mediated by polyphosphoric acid according to a known procedure.[16] We have previously reported the syntheses of naphtho[2,3-*d*]oxazole (**1**), 3-oxo-3*H*-benzo[*f*]benzopyran (**3**), 2-oxo-2*H*-benzo[*h*]benzopyran (**4**) and 6-oxo-6*H*-benzopyrano[6,7-*d*]-oxazoles **5** and **6**.[12,16,17]

Compounds **1**–**6** were used in the derivatisation of butyric acid in the presence of potassium fluoride (for **1**–**3**, **5** and **6**) or *N*,*N*′-dicyclohexylcarbodiimide (DCC)/1-hydroxybenzotriazole (HOBt, for **4**) in *N*,*N*-dimethylformamide (DMF) at room temperature,[14,19] which resulted in the ester prodrugs **7**–**12** in good yields (Table 1, Scheme 1). All compounds synthesised were fully characterised by HRMS, IR, ^{1}H and ^{13}C NMR spectroscopy. The IR spectra of **7**–**12** showed bands attributable to the stretching vibrations of the ester carbonyl group from 1718 to1749 cm^{-1}. ^{1}H NMR spectra showed signals of the butyric acid moiety, the methyl (δ = 0.93–1.02 ppm) and two methylene groups ($\delta \approx$ 1.72 and 2.49 ppm). The heterocyclic methylene groups were also visible for all compounds (δ = 4.14–5.69 ppm). The confirmation of the presence of the newly formed ester linkages was also supported by ^{13}C NMR spectral signals of the carbonyl group, which were found at δ = 172.68–173.59 ppm.

UV/Vis spectroscopic characterisation was carried out to obtain the parameters needed for monitoring the uncaging process. Absorption spectra of degassed 10^{-5} M solutions in absolute ethanol and in a methanol/4-(2-hydroxyethyl)-1-piperazineethanesulfonic acid (HEPES) buffer (80:20) solution of **7**–**12** were measured and compared to those of precursors **1**–**6**. Absorption maxima and molar absorptivities are reported in Table 1. By comparison of the absorption maxima for all compounds in both solvents, no significant changes were observed. The differences between the pairs of compounds were examined. For the naphtho-oxazole compounds **7** and **8**, the latter has a more defined band structure and an absorption maximum ca. 20 nm redshifted compared to that of **7**. A similar bathochromic shift was seen between oxobenzopyrans **9** and **10**, and no difference was found between **11** and **12**, which incorporate an oxobenzopyran chromophore fused with an oxazole. Replacement of the benzene ring in **7** by an oxopyran in **12** also resulted in a comparable absorption redshift.

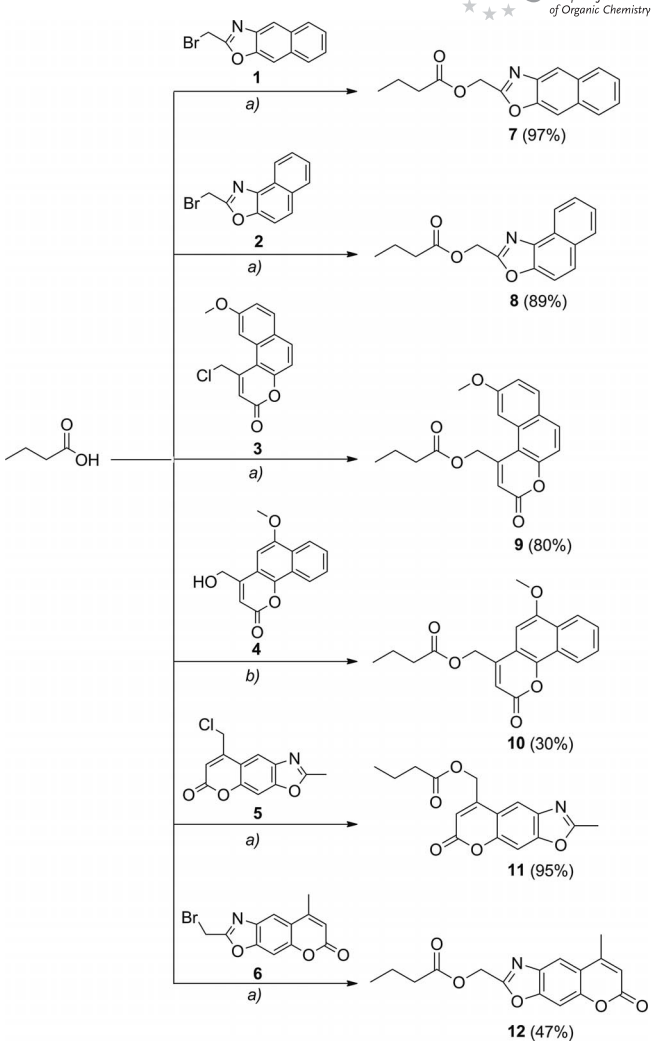

Scheme 1. Synthesis of butyric acid prodrugs **7**–**12**. (a) KF/DMF, room temp.; (b) DCC/HOBt, DMF, room temp.

The fluorescence spectra were also measured as the use of fluorescent labelling with its increased sensitivity over UV/Vis absorption techniques makes it suitable for analyti-

Table 1. Yields, UV/Vis absorption and emission data in absolute ethanol and methanol/HEPES buffer (80:20) solutions for **1**–**12**.

	Yield	Ethanol					Methanol/HEPES (80:20)				
	[%]	λ_{abs}[a]	log ε	λ_{em}[a]	Φ_F	$\Delta\lambda$[b]	λ_{abs}[a]	log ε	λ_{em}[a]	Φ_F	$\Delta\lambda$[b]
1[c]	13	334	3.67	380	0.28	3624	334	3.60	380	0.02	3624
2	98	326	3.94	355	0.22	2506	310	4.61	354	0.01	4009
3[d]	83	354	4.10	472	0.03	7062	355	3.47	458	0.10	6335
4[e]	47	365	3.69	460	0.45	5658	371	3.73	469	0.45	5632
5[c]	34	326	3.98	404	0.06	5922	325	3.94	397	0.005	5580
6[c]	23	325	3.80	424	0.01	7184	325	3.54	396	0.001	5517
7	97	300	3.52	383	0.42	7224	302	3.99	355	0.03	4944
8	89	322	3.90	355	0.11	2887	321	4.26	355	0.21	2984
9	80	350	3.92	466	0.02	7112	352	4.22	484	0.46	7748
10	30	375	3.88	474	0.38	5570	375	3.85	482	0.28	5920
11	95	325	3.96	425	0.11	7240	326	3.83	424	0.10	7090
12	47	322	3.93	457	0.03	9174	321	4.14	457	0.019	9271

[a] In nm. [b] In cm^{-1}. [c] Yield and absorption data from ref.[16] [d] Yield and absorption data in ethanol from ref.[21] [e] Yield and absorption data from ref.[17]

cal purposes. The outcome of these steady-state measurements is also given in Table 1. In recent years, the direction of the improvement of photoreleasable groups has been towards the application of polycyclic aromatic structures, which are fluorophores in most cases. However, there can be the added complication of fluorescence deactivation in some photochemical processes.

Molecules of biological importance such as butyric acid are not easily detected by UV/Vis absorption measurements and have no or low intrinsic fluorescence, and thus the introduction of a fluorophore is an appropriate strategy to enhance the photophysical properties of the resulting conjugates and to provide a means to monitor photoinduced processes. By considering the obtained values for the relative fluorescence quantum yields (Φ_F) for **7**–**12** in absolute ethanol and methanol/HEPES buffer (80:20) solution determined with 9,10-diphenylanthracene in ethanol as standard,[20] it is evident that the processes in these compounds can be monitored by fluorescence techniques. The Stokes' shifts were in the range 2506–9174 and 2984–9271 cm^{-1} in ethanol and methanol/HEPES buffer (80:20) solution, respectively, which is an advantageous property in fluorescence techniques as it will minimise self-quenching phenomena.

The photophysics of the different fluorophores in **7**–**12** in methanol/HEPES buffer (80:20) were investigated to help elucidate the processes involved upon light irradiation. Time-resolved fluorescence decays were measured at one emission wavelength (Figure 1).

Figure 1 shows the different decay behaviour for the different sets of fluorophores **7**–**12**. Compounds **7** and **8** exhibit quite complex kinetic behaviour, which is indicative of the presence of several excited states. The other compounds appear to decay in a simpler manner, although the emission from **12** is highly quenched, which is in keeping with the low quantum yield given in Table 1. The associated lifetime values extracted from the analysis of these decay curves generally reflect the trend in the quantum yields (longer lifetimes with higher quantum yields, Table 2).

To provide further insight into the processes that could be occurring in the excited state, time-resolved fluorescence measurements that monitored the emission at different wavelengths were performed to allow time-resolved emission spectra (TRES) and, by the use of global analysis, decay associated spectra (DAS) were calculated. Because of the nature of time-correlated single-photon counting, which uses very modest excitation energies (pJ per pulse), it was not envisaged that significant photocleavage would occur during the measurements. TRES for all compounds, except **9** and **10** (which bear an angular coumarin, 3-oxo-3*H*-benzo[*f*]benzopyran and 2-oxo-2*H*-benzo[*h*]benzopyran, respectively), showed changes in the spectral shape with time after excitation (Supporting Information) that hint at the presence of several species. This is in keeping with the simple time-resolved fluorescence measurements (Figure 1 and Table 2). The spectral shape of **9** and **10** appeared relatively constant, consistent with their simpler decay kinetic dominant decays of 7.4 and 9.4 ns, respectively.

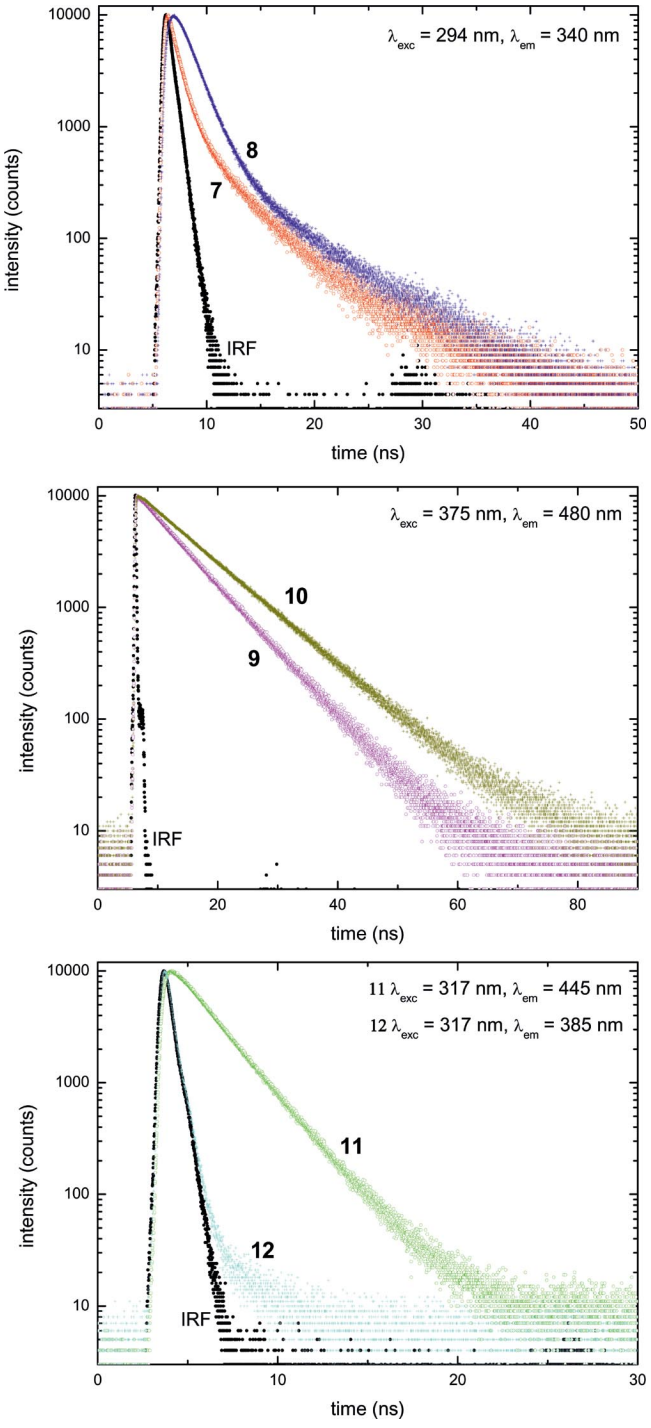

Figure 1. Fluorescence decay curves for **7**–**12**. The instrumental response function (IRF) is also shown.

Upon photolysis, it was expected that an ion pair could form, which would either undergo recombination to the ester or photocleavage.[22] Knowledge of the fluorescent species present and their kinetics may allow the rate of the photocleavage reaction to be estimated. The DAS can be useful to provide a framework to assist in this determination by providing both spectral and dynamic information. The DAS for **7**–**12** are shown in Figure 2 and were obtained from the global analysis of the time-resolved de-

Table 2. Fluorescence lifetimes (τ) for **7**–**12** obtained from reconvolution analysis of the data presented in Figure 1.[a]

	Lifetime [ns]				Relative amplitude [%]			
	τ_1	τ_2	τ_3	τ_4	f_1	f_2	f_3	f_4
7	8.04 ± 0.48	3.13 ± 0.06	0.80 ± 0.02	0.052 ± 0.009	9	23	23	45
8	6.58 ± 0.06	1.44 ± 0.01	–	–	84	16	–	–
9	7.41 ± 0.02	3.68 ± 0.12	–	–	96	4	–	–
10	9.41 ± 0.02	–	–	–	100	–	–	–
11	5.47 ± 0.31	2.12 ± 0.01	0.11 ± 0.01	–	4	87	9	–
12	1.93 ± 0.15	0.02 ± 0.01	–	–	2	98	–	–

[a] The curves were fitted to a sum of exponentials of the form $I(t) = \sum_{i}^{n} a_i\tau_i$, where a_i are normalised preexponential factors and the relative amplitude or factional (f_i) is given by $f_i = (a_i\tau_i)/(\sum_i a_i\tau_i)$.

cays taken from the TRES measurements with decays measured at 5 nm intervals. Consistent with the TRES, the behaviour of **9** and **10** appear slightly different with their emission dominated by the deexcitation of one excited state. In the case of the other compounds, global analysis shows the presence of a very short-lived decay component (and associated spectrum, because of the recovery of a clear, sensible spectral shape it is unlikely that scattered light is the origin of this decay component; a fitting artefact, although unlikely as the datasets consist of > 40 decays and the spectral

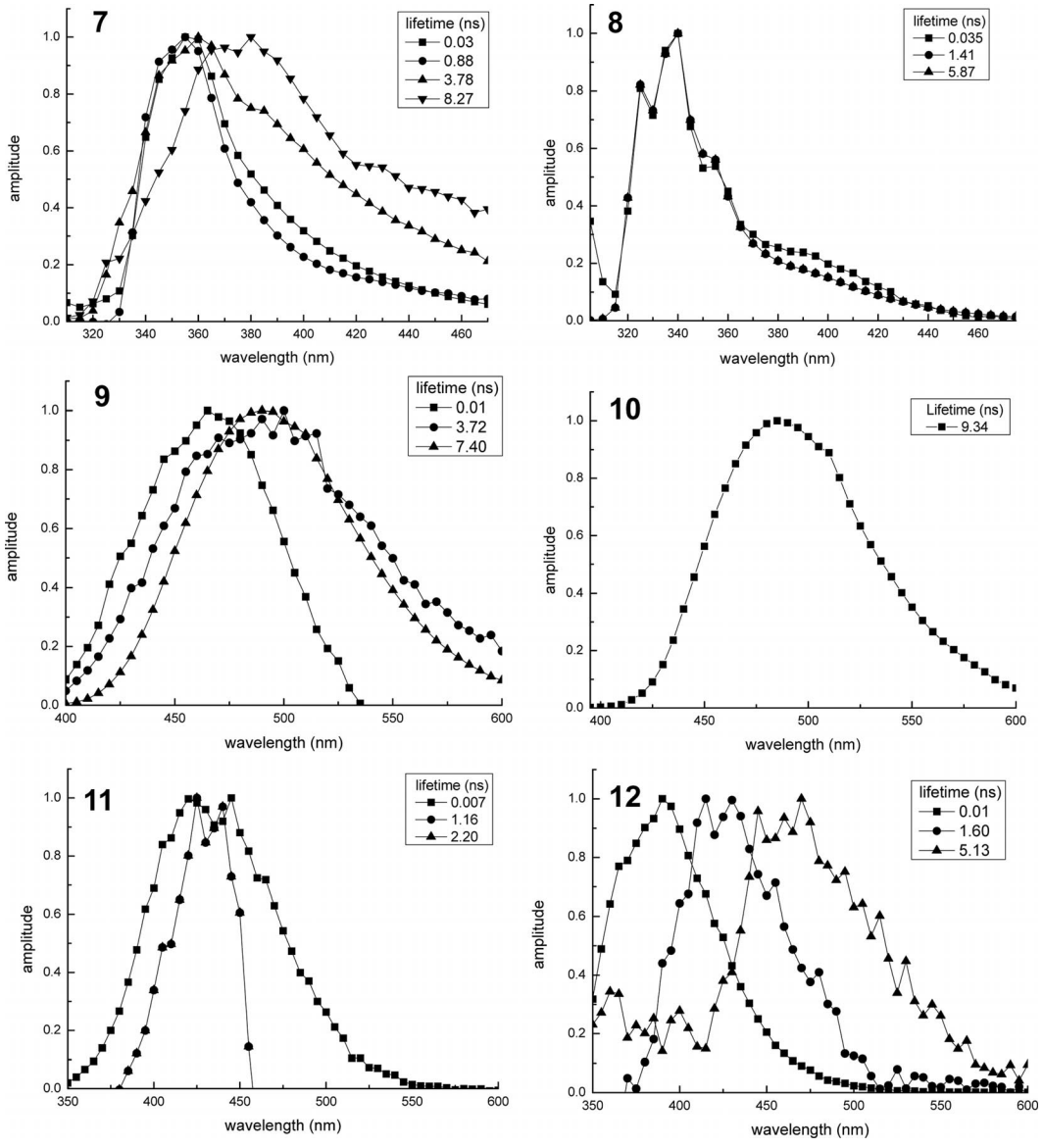

Figure 2. Normalised DAS for **7**–**12** in methanol/HEPES buffer (80:20) solution.

shape appears sensible, cannot be completely ruled out). The actual value of the shortest-lived decay should be treated with caution as it is at or beyond the resolution of the equipment and hence ought to be considered as a very short-lived decay component. The complexity of the decay behaviour of **7** and **8** may be indicative that these compounds undergo photoinduced processes more readily than the others, which can be seen later in the photolysis data and offers the possibility to monitor the whole uncaging process. The complete and rigorous attribution of the spectra and associated decay kinetics require the synthesis of appropriate model compounds for each of the chromophores. Because of the complexity seen in the fluorescence emission it can only be speculated that the shorter-lived species are those initially formed with longer lifetimes associated with the products. The complete attribution of the spectra will be left for a further study, and the results presented here demonstrate the ability of this technique to elucidate information.

Compounds **11** and **12** exhibit higher energy (shorter wavelength) spectra associated with a very fast decay and longer-lived species at longer wavelengths. This can be indicative of the longer-lived species formed from the initial formation of the species associated with the shorter-lived fluorescence. In the case of **11**, a further spectrum (ca. 1 ns) was recovered that exhibits a negative amplitude at longer wavelengths, which corresponds to the position of the 2.2 ns spectrum. Negative amplitudes for preexponentials (rise times) are commonly associated with the formation of a species in the excited state. To clearly identify the different spectra, they were normalized, and in that of **12**, the emission is completely dominated by the shorter-lived fluorescence (Table 2).

Our research into the development of alternative photosensitive groups for the protection of bifunctional molecules has involved the successful use of oxazole-based structures for the first time.[16] In addition, 2-oxo-2*H*-benzopyrans (coumarins) are well-established light-activated protecting groups, and we have been engaged in the application of their related fused derivatives, 3-oxo-3*H*-benzo[*f*]benzopyrans and 2-oxo-2*H*-benzobenzopyrans (benzocoumarins).[12,14,17,18] Both systems are suitable for photorelease purposes, their choice depends on the required wavelengths, and have encouraged us to explore their use in other applications, namely, light-triggered drug delivery.

The evaluation of photoactive butyric acid prodrugs **7**–**12**, which possess naphtho[2,3-*d*]oxazole, naphtho[1,2-*d*]-oxazole, 3-oxo-3*H*-benzo[*f*]benzopyran, 2-oxo-2*H*-benzo[*h*]-benzopyran and 6-oxo-6*H*-benzopyrano[6,7-*d*]oxazole, in which the latter has the linkage between the heterocycle and the active molecule through oxopyran or oxazole moieties, was carried out by photolysis studies under irradiation at different wavelengths. Solutions of **7**–**12** (1×10^{-4} M) in methanol/HEPES buffer (80:20) solution were irradiated with a Rayonet RPR-100 reactor at 254, 300, 350 and 419 nm in order to determine the most favourable uncaging conditions. The course of the photocleavage reaction was monitored by reverse-phase-(RP)-HPLC with UV detection. The plots of peak area (A) of the starting material vs. irradiation time (t_{irr}) were obtained for each compound at the considered wavelengths. Peak areas were determined by HPLC, which revealed a gradual decrease with time, and were the average of three runs. The determined irradiation time represents the time necessary for the consumption of the starting materials until less than 5% of the initial area was detected. Based on HPLC data for each compound, the plot of $\ln A$ vs. t_{irr} showed a linear correlation for the disappearance of the starting material, which suggests a first-order reaction and was obtained by the linear least-squares method for a straight line with good correlation coefficients. The corresponding rate constants (k) were calculated and are presented in Table 3.

Table 3. Values of t_{irr} [min] and k [$\times 10^{-2}$ min^{-1}] for the complete photolysis (>95%) of **7**–**12** at different wavelengths in methanol/HEPES buffer (80:20) solution.

	254 nm		300 nm		350 nm	
	t_{irr}	k	t_{irr}	k	t_{irr}	k
7	4.9	65.22	5.6	53.42	> 2500	–
8	0.1	2918	0.8	400	519	0.58
9	178	1.70	253	1.19	263	1.14
10	107	2.86	170	2.86	96	3.15
11	45	6.59	33	6.59	285	1.04
12	76	3.95	94	3.16	> 2500	–

By comparison of caged butyric acids **7** and **8**, which bear naphtho-oxazole units that differ in the ring fusion, a linear naphtho[2,3-*d*]oxazole and an angular naphtho[1,2-*d*]oxazole, respectively, it was found that, although both cleaved readily at 254 and 300 nm, the irradiation time obtained for the release of butyric acid from **8** was less than 1 min.

Concerning the photolysis of **7** and **8** at 350 nm, the photocleavage was not achieved in a practical period of time, which was predicted from the values of wavelengths of maximum absorption in the solvent used with the lowest irradiation time of 519 min (ca. 9 h) for **8**.

Concerning **9** and **10**, which bear angular coumarins 3-oxo-3*H*-benzo[*f*]benzopyran and 2-oxo-2*H*-benzo[*h*]benzopyran, respectively, it was found that cleavage was faster at all the wavelengths of irradiation for **10**, especially at 350 nm.

With this in mind and in order to achieve the best release conditions of butyric acid, **11** and **12**, which are based on the combination of 2-oxo-2*H*-benzopyran and oxazole in a fused system with an ester linkage to the active molecule through a methylene spacer directly connected to the pyran or oxazole rings, respectively, were studied under irradiation under the same conditions as **7**–**10**. At 254 and 300 nm, the irradiation times of **11** and **12** were longer than for **7** and **8**, whereas at 350 nm their photolytic behaviour was inferior to that of **10**, but superior to that of **7** and **8**. Comparison between the irradiation times of **11** and **12** revealed that cleavage of the ester linkage was improved for **11**, which bears butyric acid connected to the pyran ring, at all irradiation wavelengths tested. These data revealed the contribution of both heterocyclic rings when combined in a

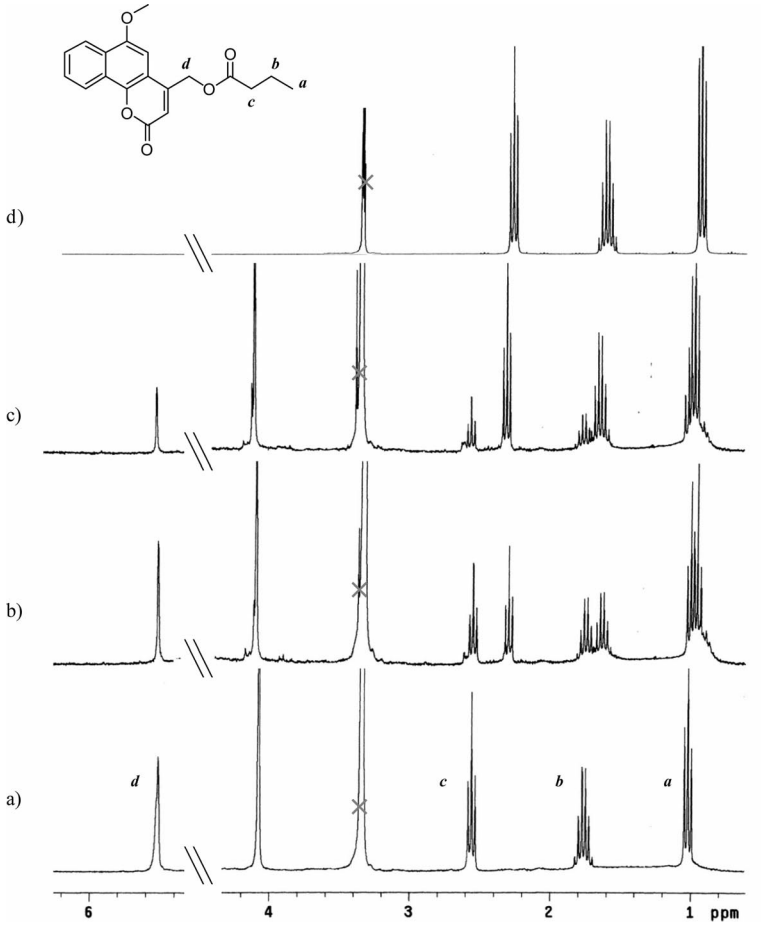

Figure 3. ^{1}H NMR spectra in [D_4]methanol/D_2O (80:20) for the photolysis of **10** at 350 nm: (a) before irradiation, (b) after irradiation for 60 min, (c) after irradiation for 140 min, (d) free butyric acid.

single system for the time required for the complete release of butyric acid from the ester cages. They are also consistent with the time-resolved fluorescence data, which indicate that the compounds that exhibit the more complex decay kinetics have the fastest rate of photocleavage.

As butyric acid is an organic molecule of biological relevance, cleavage and release could benefit from being carried out by irradiation at longer wavelengths in practical times. As a result, the behaviour of **9** and **10**, which were the most promising at 350 nm (263 min for **9** and 96 min for **10**), were also evaluated at 419 nm, which resulted in an expected increased, but still useful, irradiation time for **10** (187 min) and an impractical result for **9** (3442 min, ca. 57 h). In addition, the photolytic process at 300 nm was monitored by ^{1}H NMR in a [D_4]methanol/D_2O (80:20) solution at a concentration of 9.0×10^{-3} M (several times larger than that used in the experiments followed by HPLC), which led to an increase in the photolysis time for the complete release of the acid. During irradiation, the signals related to the linked acid decreased gradually, with concomitant increase of its signals in the released form, as well as signals due to aromatic byproducts related to the heterocyclic cage (see Figure 3 for **10** at 350 nm as a representative example). Variable irradiation times were required for the quantitative release of the butyric acid, which depended on the structure of the heterocycle.

Conclusions

Naphtho[2,3-*d*]oxazole, naphtho[1,2-*d*]oxazole, 3-oxo-3*H*-benzo[*f*]benzopyran, 2-oxo-2*H*-benzo[*h*]benzopyran and 6-oxo-6*H*-benzopyrano[6,7-*d*]oxazole (with a linkage between the heterocycle and the active molecule through oxopyran or oxazole moieties) were used in the synthesis of caged butyric acid through an ester linkage. Photolytic cleavage studies at 254, 300, 350 and 419 nm in methanol/HEPES buffer (80:20) solution revealed the possibility of using these heterocyclic systems for the light-triggered release of the active molecule in reasonable times. The use of time-resolved fluorescence techniques contributed to the elucidation of the dynamic behaviour of these systems. Overall, these results suggest that the heterocyclic cages studied may be considered as promising alternatives as photoactive prodrugs for butyric acid as a model carboxylic acid drug.

Experimental Section

General: All melting points were measured with a Stuart SMP3 melting point apparatus. TLC analyses were carried out with 0.25 mm thick precoated silica plates (Merck Fertigplatten Kieselgel $60F_{254}$), and spots were visualised under UV light. Chromatography on silica gel was carried out with Merck Kieselgel (230–240 mesh). IR spectra were determined with a BOMEM MB 104 spectrophotometer. UV/Vis absorption spectra (200–700 nm) were obtained with a Shimadzu UV/2501PC spectrophotometer. NMR spectra were obtained with a Varian Unity Plus spectrometer at an operating frequency of 300 MHz for ^{1}H and 75.4 MHz for ^{13}C or a Bruker Avance III 400 instrument at an operating frequency of 400 MHz for ^{1}H and 100.6 MHz for ^{13}C by using the solvent peak as internal reference at 25 °C. All chemical shifts are given in ppm by using $\delta_H(Me_4Si) = 0$ ppm as a reference, and J values are given in Hz. Assignments were made by comparison of chemical shifts, peak multiplicities and J values and were supported by spin decoupling-double resonance and two-dimensional heteronuclear correlation techniques. Low- and high-resolution mass spectrometry was performed at the C.A.C.T.I. – Unidad de Espectrometria de Masas, at the University of Vigo, Spain. Commercially available reagents were used as received.

Synthesis of 2-(Bromomethyl)naphtho[1,2-*d*]oxazole 2: To a solution of 1-aminonaphthalen-2-ol (0.300 g, 1.53×10^{-3} mol) in polyphosphoric acid (1.53 g) was added bromoacetic acid (0.320 g, 2.30×10^{-3} mol), and the mixture was stirred at 130 °C for 5 h. The reaction mixture was poured into iced water and stirred for 1 h to give a fine grey precipitate. The solid was collected by filtration, washed with cold water and dried in a vacuum oven. After purification by chromatography using ethyl acetate/*n*-hexane (1:1) as eluent, **2** was obtained as a grey solid (0.400 g, 98%). M.p. 106.2–107.4 °C. R_f = 0.97 (ethyl acetate/*n*-hexane, 1:1). ^{1}H NMR (300 MHz, $CDCl_3$, 25 °C): δ = 4.73 (s, 2 H, CH_2), 7.53 (dt, J = 6.9 and 1.2 Hz, 1 H, 6-H), 7.68 (dt, J = 6.9 and 1.2 Hz, 1 H, 5-H), 7.70 (d, J = 6.6 Hz, 1 H, 9-H), 7.86 (d, J = 9.0 Hz, 1 H, 7-H), 7.98 (d, J = 9.0 Hz, 1 H, 4-H), 8.48 (d, J = 6.6 Hz, 1 H, 8-H) ppm. ^{13}C NMR (75.4 MHz, $CDCl_3$, 25 °C): δ = 20.88 (CH_2), 110.81 (C-9), 121.99 (C-8), 125.67 (C-6), 126.44 (C-3a), 127.12 (C-7), 127.39 (C-5), 128.62 (C-4), 131.21 (C-3b), 136.51 (C-7a), 148.62 (C-9a), 159.95 (C-2) ppm. IR (KBr 1%): $\tilde{\nu}$ = 3100, 3055, 2974, 2924, 1700, 1656, 1600, 1500, 1392, 1309, 1275, 1254, 1218, 1102, 1049, 926, 888, 813, 743, 687, 666 cm^{-1}. HRMS (EI): calcd. for $C_{12}H_8NO^{79}Br$ [M^+] 260.9789; found 260.9778; calcd. for $C_{12}H_8NO^{81}Br$ [M^+] 262.9769; found 262.9772.

Synthesis of 7–12

General Procedure for the Synthesis of 7–9, 11 and 12: To a solution of the bromo- or chloromethyl precursor **1**–**3**, **5** and **6** (1 equiv.) in dry DMF (2 or 3 mL) were added potassium fluoride (3 equiv.) and butyric acid (1 equiv.). The reaction mixture was stirred at room temperature for 5 h or 2 d (**9**, **11** and **12**). Potassium fluoride was removed by filtration, the solvent was removed by rotary evaporation under reduced pressure and the crude residue was purified by column chromatography using mixtures of ethyl acetate and *n*-hexane as eluent.

(Naphtho[2,3-*d*]oxazol-2-yl)methyl Butyrate (7): From the reaction of **1** (0.030 g, 1.15×10^{-4} mol) in DMF (2 mL), potassium fluoride (0.020 g, 3.45×10^{-4} mol) and butyric acid (0.010 g, 1.15×10^{-4} mol), **7** was obtained as a yellow solid (0.030 g, 97%). M.p. 125.7–126.5 °C. R_f = 0.93 (ethyl acetate/*n*-hexane, 1:1). ^{1}H NMR (400 MHz, $CDCl_3$, 25 °C): δ = 1.01 (t, J = 7.6 Hz, 3 H, CH_3), 1.75 (sext, J = 7.6 Hz, 2 H, CH_2), 2.48 (t, J = 7.6 Hz, 2 H, CH_2), 5.40 (s, 2 H, CH_2 Het), 7.46–7.53 (m, 2 H, 6-H and 7-H), 7.91 (s, 1 H, 9-H), 7.95 (dd, J = 6.8 and 2.7 Hz, 1 H, 8-H), 7.99 (dd, J = 6.9 and 2.7 Hz, 1 H, 5-H), 8.18 (s, 1 H, 4-H) ppm. ^{13}C NMR (100.6 MHz, $CDCl_3$, 25 °C): δ = 13.55 (CH_3), 18.28 (CH_2), 35.66 (CH_2), 58.08 (CH_2 Het), 106.66 (C-9), 117.89 (C-4), 124.80 (C-7), 125.71 (C-6), 127.88 (C-8), 128.53 (C-5), 131.26 (C-8a), 131.70 (C-4a), 140.54 (C-3a), 149.50 (C-9a), 163.01 (C-2), 172.71 (C=O) ppm. IR (KBr 1%): $\tilde{\nu}$ = 2958, 2932, 2875, 1740, 1694, 1644, 1626, 1579, 1505, 1470, 1443, 1415, 1305, 1260, 1242, 1165, 1096, 1050, 1018, 956, 938, 900, 882, 867, 799, 767, 666 cm^{-1}. HRMS (EI): calcd. for $C_{16}H_{15}NO_3$ [M^+] 269.1052; found 269.1058.

(Naphtho[1,2-*d*]oxazol-2-yl)methyl Butyrate (8): From the reaction of **2** (0.109 g, 4.18×10^{-4} mol) in DMF (4 mL), potassium fluoride (0.073 g, 1.25×10^{-3} mol) and butyric acid (0.037 g, 4.18×10^{-4} mol), **8** was obtained as a brown oil (0.100 g, 89%). R_f = 0.98 (ethyl acetate/*n*-hexane, 1:1). ^{1}H NMR (400 MHz, $CDCl_3$, 25 °C): δ = 0.98 (t, J = 7.6 Hz, 3 H, CH_3), 1.72 (sext, J = 7.6 Hz, 2 H, CH_2), 2.43 (t, J = 7.6 Hz, 2 H, CH_2), 5.43 (s, 2 H, CH_2 Het), 7.53 (dt, J = 6.8 and 0.8 Hz, 1 H, 6-H), 7.65 (dt, J = 6.8 and 0.8 Hz, 1 H, 5-H), 7.66 (d, J = 9.2 Hz, 1 H, 9-H), 7.79 (d, J = 9.2 Hz, 1 H, 7-H), 7.94 (d, J = 9.0 Hz, 1 H, 4-H), 8.46 (d, J = 7.6 Hz, 1 H, 8-H) ppm. ^{13}C NMR (100.6 MHz, $CDCl_3$, 25 °C): δ = 13.51 (CH_3), 18.25 (CH_2), 35.67 (CH_2), 58.07 (CH_2 Het), 110.75 (C-9), 121.91 (C-8), 125.42 (C-6), 126.41 (C-3a), 126.57 (C-7), 127.12 (C-5), 128.46 (C-4), 131.05 (C-3b), 136.09 (C-7a), 148.25 (C-9a), 159.55 (C-2), 172.72 (C=O) ppm. IR (KBr 1%): $\tilde{\nu}$ = 3067, 2966, 2936, 2876, 1747, 1704, 1640, 1592, 1572, 1529, 1448, 1374, 1308, 1273, 1259, 1164, 1101, 1046, 1029, 1005, 939, 880, 804, 749, 697, 665 cm^{-1}. HRMS (EI): calcd. for $C_{16}H_{15}NO_3$ [M^+] 269.1052; found 269.1051.

(9-Methoxy-3-oxo-3*H*-benzo[*f*]benzopyran-1-yl)methyl Butyrate (9): From the reaction of **3** (0.03 g, 1.09×10^{-4} mol) in DMF (2 mL), potassium fluoride (0.019 g, 3.27×10^{-4} mol) and butyric acid (0.011 g, 1.20×10^{-4} mol), **9** was obtained as a brown solid (0.027 g, 80%). M.p. 123.7–124.9 °C. R_f = 0.58 (ethyl acetate/light petroleum, 3:7). ^{1}H NMR (400 MHz, $CDCl_3$, 25 °C): δ = 1.01 (t, J = 7.6 Hz, 3 H, CH_3), 1.74 (sext, J = 7.2 Hz, 2 H, CH_2), 2.49 (t, J = 7.6 Hz, 2 H, CH_2), 3.97 (s, 3 H, OCH_3), 5.69 (d, J = 1.6 Hz, 2 H, CH_2 Het), 6.68 (d, J = 1.6 Hz, 1 H, 2-H), 7.21 (dd, J = 8.8 and 2.4 Hz, 1 H, 8-H), 7.33 (d, J = 8.8 Hz, 1 H, 5-H), 7.48 (d, J = 2.4 Hz, 1 H, 10-H), 7.82 (d, J = 9.2 Hz, 1 H, 7-H), 7.91 (d, J = 8.8 Hz, 1 H, 6-H) ppm. ^{13}C NMR (100.6 MHz, $CDCl_3$, 25 °C): δ = 13.64 (CH_3), 18.29 (CH_2), 35.96 (CH_2), 55.43 (OCH_3), 64.01 (CH_2 Het), 105.73 (C-10), 111.98 (C-4b), 112.76 (C-2), 115.30 (C-5), 116.65 (C-8), 126.38 (C-6a), 130.64 (C-6b), 131.30 (C-7), 133.74 (C-6), 151.17 (C-1), 155.54 (C-4a), 159.66 (C-9), 160.31 (C-3), 172.76 (C=O) ppm. IR (KBr 1%): $\tilde{\nu}$ = 3416, 2964, 2931, 2252, 1718, 1625, 1595, 1518, 1461, 1444, 1425, 1406, 1363, 1335, 1299, 1277, 1231, 1198, 1105, 1060, 1023, 988, 949, 911, 846, 821, 732, 665, 646, 601 cm^{-1}. HRMS (EI): calcd. for $C_{19}H_{18}O_5$ [M^+] 326.1154; found 326.1171.

(2-Methyl-6-oxo-6*H*-benzopyrano[6,7-*d*]oxazol-8-yl)methyl Butyrate (11): From the reaction of **5** (0.029 g, 1.15×10^{-4} mol) in DMF (2 mL), potassium fluoride (0.020 g, 3.45×10^{-4} mol) and butyric acid (0.010 g, 1.15×10^{-4} mol), **11** was obtained as a yellow oily solid (0.032 g, 95%). ^{1}H NMR (300 MHz, $CDCl_3$, 25 °C): δ = 1.00 (t, J = 7.2 Hz, 3 H, CH_3), 1.74 (sext, J = 7.2 Hz, 2 H, CH_2), 2.43 (t, J = 7.2 Hz, 2 H, CH_2), 2.7 (s, 3 H, CH_3 Het), 5.36 (s, 2 H, CH_2 Het), 6.50 (s, 1 H, 7-H), 7.50 (s, 1 H, 4-H), 7.79 (s, 1 H, 9-H) ppm. ^{13}C NMR (75.4 MHz, $CDCl_3$, 25 °C): δ = 13.65 (CH_3), 14.62 (CH_3 Het), 18.34 (CH_2), 35.88 (CH_2), 61.18 (CH_2 Het), 99.58 (C-4), 112.13 (C-7), 113.44 (C-9), 114.36 (C-8a), 138.62 (C-9a), 149.55 (C-

8), 151.58 (C-4a), 152.67 (C-3a), 160.37 (C-6), 166.02 (C-2), 172.71 (C=O) ppm. IR (KBr 1%): $\tilde{\nu}$ = 3077, 3048, 3010, 2928, 1743, 1722, 1642, 1606, 1578, 1477, 1437, 1430, 1394, 1382, 1354, 1283, 1273, 1253, 1218, 1149, 1131, 1037, 1016, 962, 915, 901, 879, 869, 814, 734, 699, 681, 609 cm^{-1}. HRMS (EI): calcd. for $C_{16}H_{15}NO_5$ [M^+] 301.0951; found 301.0953.

(8-Methyl-6-oxo-6*H*-benzopyrano[6,7-*d*]oxazol-2-yl)methyl Butyrate (12): From the reaction of **6** (0.031 g, 1.05×10^{-4} mol) in DMF (2 mL), potassium fluoride (0.018 g, 3.15×10^{-4} mol) and butyric acid (0.010 g, 1.15×10^{-4} mol), **12** was obtained as a white solid (0.015 g, 47%). M.p. 118.1–119.3 °C. R_f = 0.45 (ethyl acetate/light petroleum, 3:7). ^{1}H NMR (400 MHz, $CDCl_3$, 25 °C): δ = 1.00 (t, J = 7.6 Hz, 3 H, CH_3), 1.74 (sext, J = 7.2 Hz, 2 H, CH_2), 2.48 (t, J = 7.6 Hz, 2 H, CH_2), 2.52 (d, J = 1.2 Hz, 3 H, CH_3 Het), 5.37 (s, 2 H, CH_2 Het), 6.34 (d, J = 1.2 Hz, 1 H, 7-H), 7.52 (d, J = 0.4 Hz, 1 H, 4-H), 7.96 (s, 1 H, 9-H) ppm. ^{13}C NMR (100.6 MHz, $CDCl_3$, 25 °C): δ = 13.58 (CH_3), 18.29 (CH_2), 19.21 (CH_3), 35.65 (CH_2), 57.75 (CH_2 Het), 99.64 (C-4), 114.27 (C-7), 115.63 (C-9), 117.89 (C-8a), 137.74 (C-9a), 152.0 (C-4a), 152.32 (C-8), 152.38 (C-3a), 160.40 (C-6), 162.52 (C-2), 172.68 (C=O) ppm. IR (KBr 1%): $\tilde{\nu}$ = 3054, 2960, 2931, 2878, 1788, 1737, 1717, 1631, 1569, 1437, 1404, 1385, 1368, 1341, 1316, 1280, 1241, 1210, 1167, 1130, 1053, 1028, 950, 925, 908, 877, 858, 811, 782, 755, 742, 697, 665, 642 cm^{-1}. HRMS (EI): calcd. for $C_{16}H_{15}NO_5$ [M^+] 301.0951; found 301.0931.

Synthesis of (6-Methoxy-2-oxo-2*H*-benzo[*h*]benzopyran-4-yl)methyl Butyrate (10): To a solution of **4** (0.022 g, 8.83×10^{-5} mol) in dry DMF (2 mL) at 0 °C was added HOBt (0.024 g, 2.56×10^{-4} mol) followed by DCC (0.053 g, 2.57×10^{-4} mol) after stirring for 10 min. After 10 min, butyric acid (1.6×10^{-2} mL, 1.77×10^{-4} mol) was added and the reaction mixture was stirred at room temperature for 5 d. The solvent was evaporated and the crude residue dissolved in dichloromethane (10 mL). The organic phase was washed with sodium carbonate (3 × 10 mL) and dried with magnesium sulfate. Purification by chromatography in dichloromethane/methanol (100:1) gave **10** as a yellow solid (0.009 g, 30%). M.p. 124.6–125.3 °C. R_f = 0.88 (dichloromethane/methanol, 100:1). ^{1}H NMR (400 MHz, $CDCl_3$, 25 °C): δ = 1.02 (t, J = 7.2 Hz, 3 H, CH_3), 1.72–1.81 (m, 2 H, CH_2), 2.48 (t, J = 7.2 Hz, 2 H, CH_2), 4.04 (s, 3 H, OCH_3), 5.38 (d, J = 1.2 Hz, 2 H, CH_2 Het), 6.59 (s, 1 H, 3-H), 6.65 (s, 1 H, 5-H), 7.65–7.70 (m, 2 H, 8-H and 9-H), 8.27–8.29, (m, 1 H, 7-H), 8.51–8.54 (m, 1 H, 10-H) ppm. ^{13}C NMR (100.6 MHz, $CDCl_3$, 25 °C): δ = 13.68 (CH_3), 18.41 (CH_2), 35.98 (CH_2), 55.87 (OCH_3), 61.33 (CH_2 Het), 95.27 (C-5), 112.22 (C-4a), 112.47 (C-3), 122.24 (C-7), 122.42 (C-10), 124.01 (C-10a), 127.36 (C-6a), 127.94 (C-9), 128.43 (C-8), 145.72 (C-10b), 149.86 (C-4), 152.30 (C-6), 160.80 (C-2), 172.84 (C=O) ppm. IR (KBr 1%): $\tilde{\nu}$ = 2965, 2925, 2853, 1749, 1727, 1613, 1595, 1564, 1505, 1472, 1455, 1422, 1384, 1353, 1308, 1272, 1248, 1167, 1142, 1118, 1084, 1031, 990, 956, 858, 818, 778, 735, 666 cm^{-1}. HRMS (EI): calcd. for $C_{19}H_{18}O_5$ [M^+] 326.1154; found 326.1157.

Time-Resolved Fluorescence Measurements: Time-resolved fluorescence measurements were performed with a HORIBA Scientific FluoroCube-01 equipped with DeltaDiode excitation sources (running either at 8 or 10 MHz) and a TBX-07C detector. The excitation wavelengths employed were 295 nm (LED source) for **7** and **8**, 375 nm (laser source) for **9** and **10** and 317 nm (LED source) for **11** and **12**. Data were analysed by using DAS6 software and the decays reconvoluted with the instrumental response and fitted to the sum of exponentials. The goodness of fit was judged in terms of a chi-squared value and weighted residuals. DAS, associating the spectra with a decay time, were obtained from the global analysis (by using DAS6 software) of the TRES measurements, which involved the collection of fluorescence decays for a fixed collection time over a selected wavelength range (at 5 nm intervals).

Photolysis General: Photolyses were carried out by using a Rayonet RPR-100 chamber reactor equipped with 10 lamps of 254, 300, 350 and 419 nm. HPLC analyses were performed by using a Licrospher 100 RP18 (5 μm) column in a JASCO HPLC system composed by a PU-2080 pump and a UV-2070 detector with ChromNav software.

Photolysis Procedure: A 1×10^{-4} M methanol/HEPES buffer (80:20) solution of **7**–**12** (5 mL) was placed in a quartz tube and irradiated in the reactor at the desired wavelength. HEPES buffer solution was prepared in distilled water with HEPES (10 mM), sodium chloride (120 mM), potassium chloride (3 mM), calcium chloride (1 mM) and magnesium chloride (1 mM) and pH adjusted to 7.2. Aliquots of 100 μL were taken at regular intervals and analysed by RP-HPLC. The eluent was acetonitrile/water (3:1) at a flow rate of 0.8 (**7–9**, **12**) or 1.0 mL/min (**10**, **11**) previously filtered through a Millipore type HN 0.45 μm filter and degassed by ultrasound for 30 min. The chromatograms were traced by detecting UV absorption at the wavelength of maximum absorption for each conjugate (retention time: **7**, 7.4; **8**, 7.7; **9**, 6.6; **10**, 8.6; **11**, 6.4; **12**, 4.2 min).

Supporting Information (see footnote on the first page of this article): Time-resolved emission spectra (TRES) for compounds **7**–**12** in methanol/HEPES buffer (80:20) solution.

Acknowledgments

Thanks are due to the Fundação para a Ciência e Tecnologia (Portugal) for financial support through project PTDC/QUI/69607/2006 (FCOMP-01-0124-FEDER-007449) and PhD grants to A. M. P. (SFRH/BD/61459/2009) and A. M. S. S. (SFRH/BD/80813/2011). The Bruker Avance III 400 NMR spectrometer is part of the National NMR Network (RNRMN) and was purchased in the framework of the National Program for Scientific Re-equipment, contract REDE/1517/RMN/2005 with funds from POCI 2010 (FEDER) and FCT.

[1] V. J. Stella, R. T. Borchardt, M. J. Hageman, R. Oliyai, H. Maag, J. W. Tilley in *Prodrugs: Challenges and Rewards*, part 1, vol. V, Springer, New York, **2007**, pp. 703–729.
[2] A. S. Kearney, *Adv. Drug Delivery Rev.* **1996**, *19*, 225–239.
[3] B. Pavan, A. Dalpiaz, N. Ciliberti, C. Biondi, S. Manfredini, S. Vertuani, *Molecules* **2008**, *13*, 1035–1065.
[4] Z. Zhang, H. Hatta, T. Ito, S. Nishimoto, *Org. Biomol. Chem.* **2005**, *3*, 592–596.
[5] M. S. Kim, S. L. Diamond, *Bioorg. Med. Chem. Lett.* **2006**, *16*, 4007–4010.
[6] G. Berkovitch, D. Doron, A. Nudelman, Z. Malik, A. Rephaeli, *J. Med. Chem.* **2008**, *51*, 7356–7369.
[7] P. R. Pouillart, *Life Sci.* **1998**, *63*, 1739–1760.
[8] L. Spina, F. Cavallaro, N. I. Fardowza, P. Lagoussis, D. Bona, C. Ciscato, A. Rigante, M. Vecchi, *Digest. Liver Dis. Supp.* **2007**, *1*, 7–11.
[9] I. Levovich, A. Nudelman, G. Berkovitch, L. Swift, S. Cutts, D. R. Phillips, A. Rephaeli, *Cancer Chemother. Pharmacol.* **2008**, *62*, 471–482.
[10] A. Brioschi, G. P. Zara, S. Calderoni, M. R. Gasco, A. Mauro, *Molecules* **2008**, *13*, 230–254.
[11] U. Aich, M. A. Meledeo, S.-G. Sampathkumar, J. Fu, M. B. Jones, C. A. Weier, S. Y. Chung, B. C. Tang, M. Yang, J. Hanes, K. J. Yarema, *Glycoconjugate J.* **2010**, *27*, 445–459.
[12] A. M. Piloto, D. Rovira, S. P. G. Costa, M. S. T. Gonçalves, *Tetrahedron* **2006**, *62*, 11955–11962.

[13] A. S. C. Fonseca, M. S. T. Gonçalves, S. P. G. Costa, *Tetrahedron* **2007**, *63*, 1353–1359.
[14] M. J. G. Fernandes, M. S. T. Gonçalves, S. P. G. Costa, *Tetrahedron* **2008**, *64*, 3032–3038.
[15] A. S. C. Fonseca, M. S. T. Gonçalves, S. P. G. Costa, *Amino Acids* **2010**, *39*, 699–712.
[16] A. M. S. Soares, S. P. G. Costa, M. S. T. Gonçalves, *Tetrahedron* **2010**, *66*, 8189–8195.
[17] A. M. S. Soares, S. P. G. Costa, M. S. T. Gonçalves, *Amino Acids* **2010**, *39*, 121–133.
[18] A. M. Piloto, A. M. S. Soares, S. P. G. Costa, M. S. T. Gonçalves, *Amino Acids* **2011**, DOI: 10.1007/s00726-011-0969-0.
[19] F. S. Tjoeng, G. A. Heavner, *Synthesis* **1981**, 897–899.
[20] J. V. Morris, M. A. Mahaney, J. R. Huber, *J. Phys. Chem.* **1976**, *80*, 969–974.
[21] A. M. Piloto, S. P. G. Costa, M. S. T. Gonçalves, *Tetrahedron Lett.* **2005**, *46*, 4757–4760.
[22] R. Schmidt, D. Geissler, V. Hagen, J. Bendig, *J. Phys. Chem. A* **2007**, *111*, 5768–5774.

Received: September 23, 2011
Published Online: December 8, 2011

